

This is the postprint version of the following article: *Grinyte R, Saa L, Garai-Ibabe G, Pavlov V. Biocatalytic etching of semiconductor cadmium sulfide nanoparticles as a new platform for the optical detection of analytes. Chem Commun. 2015;51(96):17152-17155*, which has been published in final form at [10.1039/c5cc05613f](https://doi.org/10.1039/c5cc05613f). This article may be used for non-commercial purposes in accordance with RSC Terms and Conditions for Self-Archiving.

## Biocatalytic etching of semiconductor cadmium sulfide nanoparticles as a new platform for optical detection of analytes

Received 00th January 20xx,  
Accepted 00th January 20xx

R. Grinyte,<sup>a</sup> L. Saa,<sup>a</sup> G. Garai-Ibabe<sup>a</sup> and V. Pavlov<sup>a</sup>

DOI: 10.1039/x0xx00000x

**We report for the first time enzymatic etching of cadmium sulfide nanoparticles (CdS NPs). Fluorescence of semiconductor CdS NPs is modulated irreversibly by the enzymatic reaction catalyzed with horseradish peroxidase (HRP). We observed blue-shifts of corresponding fluorescence peak for CdS NPs and decrease in the intensity of the fluorescence signal.**

www.rsc.org/

In bioanalysis detection of analytes of interest is performed using specific interactions of biological recognition elements.<sup>1</sup> A recognition event should be transduced into some weak measurable signal which requires frequently amplification.<sup>2</sup> Metallic nanoparticles (NPs)<sup>3</sup> and semiconductor nanoparticles (SNPs) can be very conveniently employed for signal transduction by physical methods. Their chemical and physical properties are defined by three dimensional structures of NPs, therefore very slight changes in shape and size lead to drastic variation in absorption and emission spectra. Usually, pre-synthesized semiconductor NPs are tethered to an analyte through recognition elements report a recognition event as labels *via* optical<sup>4</sup>, electrochemical<sup>5</sup> or acoustic signal detection.<sup>6</sup> In another biosensing strategy semiconductor cadmium sulfide NPs are employed as light harvesting elements in electrochemical biosensors.<sup>7</sup> Another strategy pioneered by our group is the enzymatic growth of semiconductor quantum dots (QDs). It was demonstrated that S<sup>2-</sup> ions, thiolated products or orthophosphate generated through enzymatic reactions interact with exogenously added Cd<sup>2+</sup> to yield CdS QDs. Assays using enzymatic generation of QDs can be broken down to two major groups. The first group employs enzymatic reactions which lead to formation of H<sub>2</sub>S.<sup>8-10</sup> The second group of QDs-generating fluorogenic enzymatic assays developed by us relies on modulating the growth of CdS QDs with the products of biocatalytic transformation through inhibition or enhancement of crystallization rate.<sup>11-14</sup>

In those assays enzymes were used to generate components forming CdS QDs but the opposite process of enzymatic etching of semiconductor NPs has never been achieved. Etching technology is considered to be a particularly important process to resize semiconductor NPs and to tune their luminescence properties. However, very harsh conditions and dangerous oxidizing agents are usually required for oxidation of semiconductor materials.<sup>15, 16</sup> Previously we reported enzymatic etching of gold NPs where free radicals produced by the enzyme horseradish peroxidase (HRP) etch gold NPs in the presence of Br<sup>-</sup> anions and H<sub>2</sub>O<sub>2</sub>.<sup>17</sup> Etching of gold nanorods triggered by different analytes recently became a very promising platform for optical detection of a number of targets including H<sub>2</sub>O<sub>2</sub>, Cu<sup>2+</sup>, Pb<sup>2+</sup>, Fe<sup>3+</sup>, Cr(VI), Co<sup>2+</sup>, CN<sup>-</sup>, I<sup>-</sup>, Cl<sup>-</sup>, NO<sub>2</sub><sup>-</sup> and glucose.<sup>17-27</sup>

HRP is available and inexpensive enzyme extensively used in biology and biotechnology for its unique characteristics.<sup>28, 29</sup> This enzyme can catalyze the oxidation of various chromogenic substrates such as 3,3',5,5'-tetramethylbenzidine (TMB), 2,3-dimethoxyphenol, guaiacol, 5-amino-2,3-dihydro-1,4-phthalazinedione (luminol), 2,2'-azino-bis(3-ethylbenzothiazoline-6-sulfonate) (ABTS), and even oxidation of species having high standard redox potential such as gold atoms of NPs.

As far as we know oxidation of semiconductor CdS NPs catalyzed by redox enzymes such as HRP has never been reported. Here we demonstrate that HRP also is able to catalyze the etching of semiconductor NPs.

In the present article, we report a facile, fast and straightforward enzymatic etching process of CdS NPs by HRP in the presence of H<sub>2</sub>O<sub>2</sub>. We prepared CdS NPs by rapid procedure used by us in previous works.<sup>10</sup> A certain amount of sulfide ions was mixed with 37 fold excess of cadmium ions at room temperature in low acidic citrate buffer. After 5 min incubation stable fluorescent CdS NPs were obtained. The obtained CdS NPs were subjected to the action of different concentrations of H<sub>2</sub>O<sub>2</sub> in the presence of fixed quantity of

<sup>a</sup> CIC biomaGUNE, Parque Tecnológico de San Sebastián, Paseo Miramón 182, 20009, San Sebastián (Spain)  
Tel. +34943005308; Fax +34943005314  
E-mail: vpavlov@cicbiomagune.es.

† Electronic Supplementary Information (ESI) available: experimental data, additional emissions spectra and control experiments. See DOI: 10.1039/x0xx00000x

HRP. It was found out that the treatment of CdS NPs with varying concentrations of  $\text{H}_2\text{O}_2$  in the presence of fixed amount of HRP and sodium bromide leads to the decrease in the intensity of emission peaks corresponding to semiconductor CdS NPs (Figure 1). The loss of fluorescence shows that amount of CdS NPs present in the reaction mixture is diminishing in the course of enzymatic oxidation. It is important to note that in the absence of HRP no significant changes in the emission spectra of CdS NPs were noticed in concentration range of  $\text{H}_2\text{O}_2$  up to 0.2 mM. So the decrease in the fluorescence was not caused by possible quenching effect of  $\text{H}_2\text{O}_2$ . At the same time the position of peaks was shifted from 489 to 479 (Figure 1B, inset). As it has been described in the literature<sup>30</sup> the blue shift of emission peaks reveals that the particles were etched and the size decrease is directly related with the concentration of  $\text{H}_2\text{O}_2$ . Both calibration curves shown in Figure 1B demonstrated linearity from 0 to 0.05 mM and saturation starting from 0.2 mM of  $\text{H}_2\text{O}_2$  concentration. The decrease in the fluorescence and shift of the fluorescence peak were directly related with quantity of the enzymatic substrate,  $\text{H}_2\text{O}_2$ , in the reaction mixture.

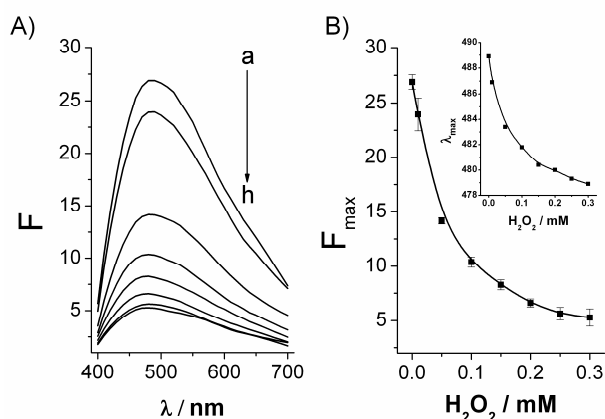


**Fig. 1.** (A) Fluorescence emission spectra of the system containing CdS NPs, HRP (2.5  $\mu\text{M}$ ), NaBr (8 mM) and different concentrations of  $\text{H}_2\text{O}_2$ : a) 0 mM; b) 0.01 mM; c) 0.05 mM; d) 0.1 mM; e) 0.15 mM; f) 0.2 mM; g) 0.25 mM; h) 0.3 mM; (B) Calibration curve of  $\text{H}_2\text{O}_2$  obtained using maximum fluorescence intensity of the peak,  $F_{\text{max}}$ . Inset: the position of emission peaks at different concentrations of  $\text{H}_2\text{O}_2$ .

According to the shape of both calibration curves oxidation of CdS NPs with  $\text{H}_2\text{O}_2$  catalysed by HRP follows the classical Michaelis-Menten kinetic model describing the initial bimolecular reaction between enzyme and the substrate. The experimental data were fitted by non linear regression method according to the Michaelis-Menten equation  $\Delta F = \Delta F_{\text{max}} [\text{H}_2\text{O}_2] / (K_M + [\text{H}_2\text{O}_2])$ ,  $K_M$  is the apparent Michaelis-Menten constant equal to  $57.2 \pm 5.2 \mu\text{M}$ . The value of  $K_M$  for  $\text{H}_2\text{O}_2$  measured using TMB as the substrate under the same experimental conditions was  $1300 \mu\text{M}$ . This difference in apparent Michaelis-Menten constants indicates that oxidation of CdS NPs proceeds through dissociation:  $\text{CdS} \rightleftharpoons \text{Cd}^{2+} + \text{S}^2$ . In accordance with the calibration curve (Figure 1B) the limit of  $\text{H}_2\text{O}_2$  detection was calculated to be  $8 \mu\text{M}$  by UPAC

definition.<sup>31</sup> This detection limit is 5 times lower than that reported for detection of  $\text{H}_2\text{O}_2$  using the enzymatic growth of CdS NPs.<sup>10</sup>

In order to elucidate further the mechanism of enzymatic oxidation of CdS NPs the effect of varying concentrations of HRP on the observed fluorescence intensity was studied. The reaction was carried out at the constant concentration of hydrogen peroxide equal to 0.2 mM in the presence of sodium bromide.

Figure S1 (ESI) shows the evolution of emission spectra of CdS NPs during the etching process in the presence of increasing concentrations of HRP. We observed that decrease in the fluorescence signal and blue shifts of emission peaks (Figure S1B, inset) are directly related with the increase in the concentration of HRP. Given the fact that in the presence of 2.5  $\mu\text{M}$  HRP without  $\text{H}_2\text{O}_2$  no effect on the fluorescence of CdS NPs was detected (as one can see in Figure 1) the fluorescence loss is caused by the biocatalytic reaction.

Statistical analysis from transmission electron microscopy (TEM) images was used to analyze the diameter of the CdS NPs before and after biocatalytic oxidation. As demonstrated in Figure 2A and B the particle diameter and concentration of CdS NPs decreased due to etching. Furthermore, size distribution plots revealed that before etching the particles had the medium diameter around 2.8 nm (Figure 2C). However, upon addition of  $\text{H}_2\text{O}_2$  the medium diameter of CdS NPs reduced by almost 2 times (Figure 2D).

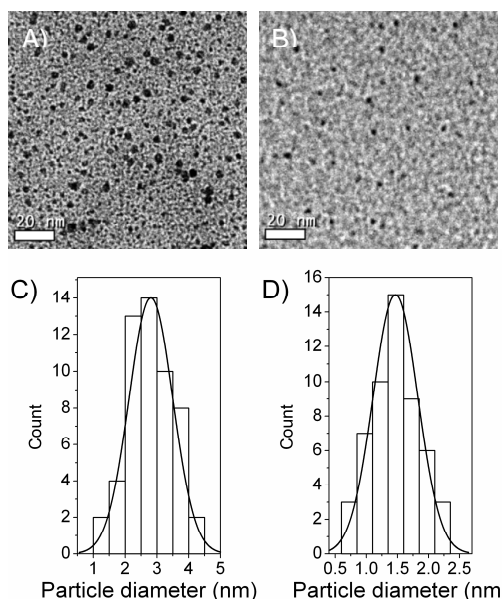
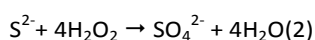
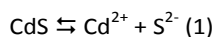


**Fig. 2.** TEM images of CdS NPs (A) before (B) after etching; Size distribution of CdS NPs (C) before (D) after etching.

Since the etching reaction did not proceed in the absence of sodium bromide some additional experiments were performed. The influence of varying bromide concentrations on the emission spectrum of CdS NPs was studied. In the absence of  $\text{H}_2\text{O}_2$  and HRP the fluorescence intensity was not significantly changed up to 8 mM of NaBr and then linearly decreased (Figure S2 curve a). We also examined the effect of

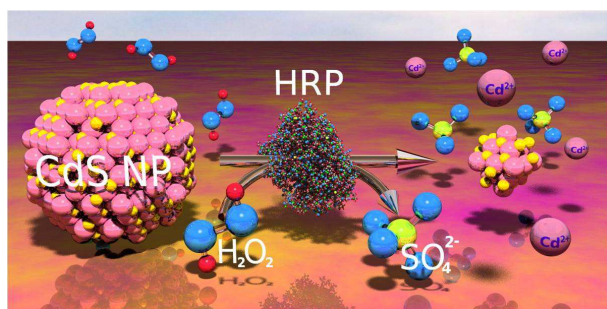
bromide concentration on the process of enzymatic etching (Figure S2 curve b). At fixed concentration of HRP and  $\text{H}_2\text{O}_2$  the increase in the bromide concentration resulted in rapid acceleration of etching rate up to 8 mM of NaBr. This optimized bromide concentration (8 mM) was used in the previous experiments of enzymatic etching.

Other halides such as chloride, iodide and fluoride did not influence the etching rate (Figure S3). This observation corroborates well with the previously published finding that  $\text{Cd}^{2+}$  is able to form  $[\text{CdBr}_4]^{2-}$  complex with  $\text{Br}^-$  ions.<sup>32</sup> The formation of  $[\text{CdBr}_4]^{2-}$  favours oxidation of CdS nanoparticles through sequestering free  $\text{Cd}^{2+}$  cations produced in the course of enzymatic reaction. The driving force of the etching process is biocatalytic oxidation of  $\text{S}^{2-}$  yielding  $\text{SO}_4^{2-}$  ions according to the Equation 1 and 2:



The formation of sulfate ions was confirmed by two independent methods. We employed capillary electrophoresis (CE) (Figure S4) to determine sulfate ions in the filtrate of CdS NPs before and after etching at optimum concentrations of HRP,  $\text{H}_2\text{O}_2$  and sodium bromide. Sulfate ions were detected only in the filtered reaction mixture obtained after biocatalytic oxidation. No sulfate ions were discovered in the filtered reaction mixture which was not subjected to enzymatic reaction. Another independent method was based on the classical specific analytical reaction between  $\text{SO}_4^{2-}$  and  $\text{Ba}^{2+}$  ions resulting in insoluble  $\text{BaSO}_4$  particles determined by UV-vis spectroscopy Figure S5. This classical analytical assay also confirmed presence of  $\text{SO}_4^{2-}$  only in the filtrate of reaction mixtures composed of CdS NPs, HRP,  $\text{H}_2\text{O}_2$  and  $\text{Br}^-$ .

In the light of the above mentioned experiments we propose the following scheme describing biocatalytic oxidation of CdS NPs with  $\text{H}_2\text{O}_2$  and HRP (Scheme 1). HRP catalyzes oxidation of  $\text{S}^{2-}$  ions in CdS NPs by  $\text{H}_2\text{O}_2$  resulting in the formation of sulfate anions and  $\text{Cd}^{2+}$  cations.



Scheme 1. Enzymatic etching of CdS NPs.

In order to check out how the etching process can be influenced by immobilization of CdS NPs on a substrate this semiconductor NPs were immobilized on the surface of polyvinyl chloride-amine microspheres. Immobilization was performed by adsorption of negatively charged CdS NPs, stabilized with citrate, on the beads bearing positively charged amino groups. Modified beads were washed with citrate buffer. Microspheres carrying CdS NPs were employed as

substrates in the enzymatic etching reaction. The same etching phenomenon was observed as in the above-mentioned experiments with free CdS NPs (Figure 3). The apparent Michaelis-Menten constant for  $\text{H}_2\text{O}_2$  calculated from the curve in Figure 3B was  $21.6 \pm 3.1 \mu\text{M}$  (two times less than that calculated for free CdS NPs).

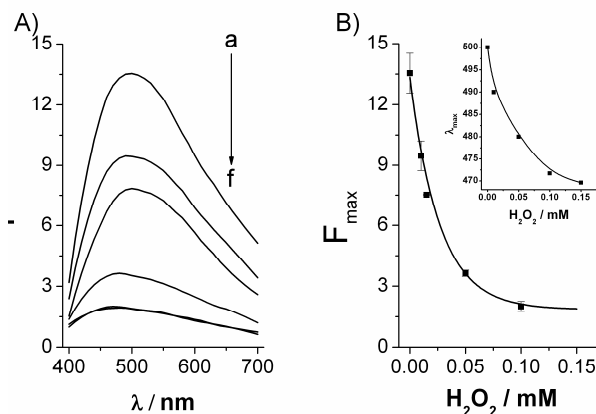


Fig. 3. (A) Fluorescence emission spectra of the system containing polyvinyl chloride microsphere-amine/CdS NPs composites, HRP (2.5  $\mu\text{M}$ ), NaBr (8 mM) and different concentrations of  $\text{H}_2\text{O}_2$ : a) 0 mM; b) 0.01 mM; c) 0.015 mM; d) 0.05 mM; e) 0.1 mM; f) 0.15 mM. (B) Calibration curve of  $\text{H}_2\text{O}_2$  obtained using maximum fluorescence intensity of the peak,  $F_{\text{max}}$ . Inset: the position of emission peaks at different concentrations of  $\text{H}_2\text{O}_2$ .

This difference can be explained by steric hindrance partially preventing dissociation of immobilized CdS NPs into  $\text{S}^{2-}$  and  $\text{Cd}^{2+}$  ions. In accordance with the calibration curve (Figure 3 B) for  $\text{H}_2\text{O}_2$  the IUPAC detection limit was found to be 7  $\mu\text{M}$  and this value is almost the same than in the experiments with free CdS NPs. The position of the peak was shifted from 500 to 470 (Figure 3. inset) indicating the evident decrease in size of immobilized CdS NPs caused by etching.

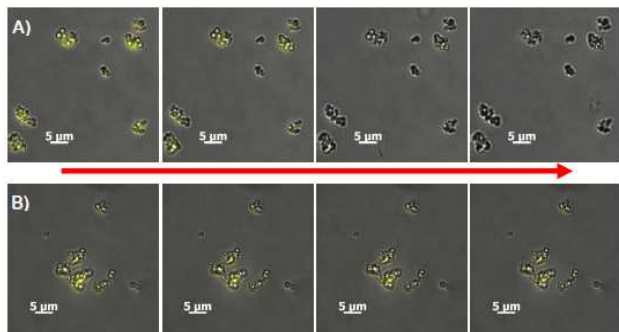
In addition, Figure S6 shows the fluorescence spectra of polyvinyl chloride-amine microspheres/CdS NPs composites after etching in the presence of fixed amount of NaBr,  $\text{H}_2\text{O}_2$  and different concentrations of HRP. In this case, we observed that increase in amounts of enzyme was correlated with decrease in emission peak intensity (Figure S6 B). As in the experiments with CdS NPs only, the same etching process was monitored after biocatalytic reaction: the peak was shifted and its intensity decreased. In conclusion, CdS immobilized microspheres could be used as nanosensors in the assay for HRP activity as described in Scheme S1 (ESI).

TEM image confirms the presence of CdS NPs on the surface of microspheres (Figure S7). As one can see in Figure S7 C, no traces of CdS NPs were detected on the surface of the beads after biocatalytic etching. It means that during biocatalytic oxidation reaction CdS NPs were etched and lost the link with microspheres or dissolved completely.

TEM images of polyvinyl chloride-amine microspheres/CdS NPs composites show dense distribution of CdS NPs on the surface of microspheres, as a result, it was possible to detect fluorescence of the immobilized QDs. For fluorescence imaging analysis wide field fluorescence microscope was used. For the

first time the changes in fluorescence in real time during the etching process were monitored by microscope (Figure 4). As shown in Figure 4, fluorescence on the surface of microspheres was completely lost after 15 min. Figure 4 B shows that in the absence of HRP no significant changes in fluorescence intensity were observed.

**Fig. 4.** Fluorescence microscope images during the etching process (A) polyvinyl



chloride microsphere-amine/CdS NPs composites in the presence of NaBr, HRP, H<sub>2</sub>O<sub>2</sub> (B) without HRP. The process was recorded during 15 min and pictures were obtained every 5 min.

Polyvinyl chloride microsphere-amine/CdS NPs composites, were applied to detection of H<sub>2</sub>O<sub>2</sub> (which is used as pre-oxidant in municipal water treatment) in tap drinking water spiked with H<sub>2</sub>O<sub>2</sub>. The recovery of this system (Table S1) was close to 100% which indicates that enzymatic etching is suitable for detection of hydrogen peroxide in real samples. The latest comparable methods for detection of H<sub>2</sub>O<sub>2</sub> using Prussian blue on polyaniline coated halloysite nanotubes or nanoporous Ag@BSA composite microspheres<sup>33,34</sup> have similar detection limit, reproducibility and selectivity but the preparation of microsphere-amine/CdS NPs composites is much simpler. The proposed method was also used to assay hydrogen peroxide in rain water as described in supplementary information. Taking into consideration all dilutions of the samples, the found concentration of H<sub>2</sub>O<sub>2</sub> in rain water was  $0.0261 \pm 0.0011$  mM Figure S8 and it lies within the range of conventional HRP-ABTS enzymatic assay  $0.0274 \pm 0.0052$  mM but our assay showed with better reproducibility with the standard deviation lower by about 5 times.

In summary, the present approach describes a facile, mild and inexpensive enzymatic etching method for resizing of CdS NPs. It was found out that the biocatalytic process involving bromide, HRP and H<sub>2</sub>O<sub>2</sub> decreased the size of semiconductor CdS NPs. Thus, this phenomenon can be applied to resizing of semiconductor CdS NPs under mild physiological conditions and rapid and sensitive detection of H<sub>2</sub>O<sub>2</sub> and HRP. It was proven that also CdS NPs immobilized on polyvinyl chloride microspheres can be etched biocatalytically. We introduce a new platform for optical detection of analytes based on etching of semiconductor NPs. Given the fact that etching of gold NPs became the basis of various analytical assays for metal ions, glucose, H<sub>2</sub>O<sub>2</sub> etc.<sup>17-27</sup> we believe that phenomenon discovered by us will find broad applications in analytical chemistry. This finding opens new path for enzymatic modification and modulation of bioelectronic devices based on semiconductor NPs.

This work was supported by the Spanish Ministry of Economy and Competitiveness (project BIO2014-59741-R) and Diputación Foral de Gipuzkoa program Redes 92/14.

## Notes and References

1. A. Ivask, T. Green, B. Polyak, A. Mor, A. Kahru, M. Virta and R. Marks, *Biosens. Bioelectron.*, 2007, **22**, 1396-1402.
2. K. Jia, M. Y. Khaywah, Y. Li, J. L. Bijeon, P. M. Adam, R. Deturche, B. Guelorget, M. Francois, G. Louarn and R. E. Ionescu, *ACS Appl. Mater. Interfaces*, **6**, 219-227.
3. S. Wu, P. Liang, H. Yu, X. Xu, Y. Liu, X. Lou and Y. Xiao, *Anal. Chem.*, **86**, 3461-3467.
4. E. Morales-Narvaez, H. Monton, A. Fomicheva and A. Merkoci, *Anal. Chem.*, **84**, 6821-6827.
5. M. Medina-Sanchez, S. Miserere, E. Morales-Narvaez and A. Merkoci, *Biosens. Bioelectron.*, **54**, 279-284.
6. E. Katz and I. Willner, *Angewandte Chemie International ed*, 2004, **43**, 6042-6108.
7. E. Katz, M. Zayats, I. Willner and F. Lisdat, *Chem. Commun.* 2006, 1395-1397.
8. L. Saa, A. Virel, J. Sanchez-Lopez and V. Pavlov, *Chemistry*, 2010, **16**, 6187-6192.
9. L. Saa, J. M. Mato and V. Pavlov, *Anal. Chem.*, 2012, **84**, 8961-8965.
10. L. Saa and V. Pavlov, *Small*, 2012, **8**, 3449-3455.
11. G. Garai-Ibabe, L. Saa and V. Pavlov, *Anal. Chem.*, 2013, **85**, 5542-5546.
12. G. Garai-Ibabe, L. Saa and V. Pavlov, *Analyst*, 2014, **139**, 280-284.
13. N. Malashikhina, G. Garai-Ibabe and V. Pavlov, *Anal. Chem.*, 2013, **85**, 6866-6870.
14. G. Garai-Ibabe, M. Moller and V. Pavlov, *Anal. Chem.*, 2012, **84**, 8033-8037.
15. H. Matsumoto, T. Sakata, H. Mori and H. Yoneyama, *J. Phys. Chem. B*, 1996, **100**, 13781-13785.
16. Y. Wang, Z. Tang, M. A. Correa-Duarte, I. Pastoriza-Santos, M. Giersig, N. A. Kotov and L. M. Liz-Marzan, *J. Phys. Chem. B*, 2004, **108**, 15461-15469.
17. L. Saa, M. Coronado-Puchau, V. Pavlov and L. M. Liz-Marzan, *Nanoscale*, 2014, **6**, 7405-7409.
18. Y. Xia, J. Ye, K. Tan, J. Wang and G. Yang, *Anal. Chem.*, 2013, **85**, 6241-6247.
19. R. Liu, Z. Chen, S. Wang, C. Qu, L. Chen and Z. Wang, *Talanta*, 2013, **112**, 37-42.
20. F.-M. Li, J.-M. Liu, X.-X. Wang, L.-P. Lin, W.-L. Cai, X. Lin, Y.-N. Zeng, Z.-M. Li and S.-Q. Lin, *Sens. and Actuators B: Chem.*, 2011, **155**, 817-822.
21. J.-M. Liu, L. Jiao, M.-L. Cui, L.-P. Lin, X.-X. Wang, Z.-Y. Zheng, L.-H. Zhang and S.-L. Jiang, *Sens. and Actuators B: Chem.*, 2013, **188**, 644-650.
22. Z. Chen, Z. Zhang, C. Qu, D. Pan and L. Chen, *Analyst*, 2012, **137**, 5197-5200.
23. R. Zou, X. Guo, J. Yang, D. Li, F. Peng, L. Zhang, H. Wang and H. Yu, *CrystEngComm*, 2009, **11**, 2797-2803.
24. Y.-Y. Chen, H.-T. Chang, Y.-C. Shiang, Y.-L. Hung, C.-K. Chiang and C.-C. Huang, *Anal. Chem.*, 2009, **81**, 9433-9439.
25. L. Shang, L. Jin and S. Dong, *Chem. Commun.*, 2009, 3077-3079.
26. S. K. Tripathy, J. Y. Woo and C. S. Han, *Anal. Chem.*, 2011, **83**, 9206-9212.
27. Z. Zhang, Z. Chen, D. Pan and L. Chen, *Langmuir*, 2015, **31**, 643-650.
28. A. M. Azevedo, V. C. Martins, D. M. Prazeres, V. Vojinovic, J. M. Cabral and L. P. Fonseca, *Biotechnology annual review*, 2003, **9**, 199-247.
29. N. C. Veitch, *Phytochemistry*, 2004, **65**, 249-259.
30. J. Liu, X. Yang, K. Wang, D. Wang and P. Zhang, *Chem. Commun.*, 2009, 6080-6082.
31. A. D. McNaught and A. Wilkinson, *Journal*, 1997, **2nd ed.**
32. R. W. Ramette, *Anal. Chem.*, 1983, **55**, 1232-1236.
33. Q. Sheng, D. Zhang, Q. Wu, J. Zheng and H. Tang, *Anal. Methods*, 2015, **7**, 6896-6903.
34. Q. Liu, T. Zhang, L. Yu, N. Jia and D.-P. Yang, *Analyst*, 2013, **138**, 5559-5562.